J. T. K. L.
JURNAL TEKNIK KIMIA DAN LINGKUNGAN

J. Tek. Kim. Ling. 2026, 10 (1), 75-90
p-ISSN : 2579-8537, e-ISSN : 2579-9746
http://jurnal.polinema.ac.id/index.php/jtkl
DOI: http://dx.doi.org/10.33795/jtkl.v10i1.8807

Biogas Generation from Liquid Waste of Tapioca Starch Processing via a Single Stage of Anaerobic Digestion and Microbial Electrolysis Cell: The Effect of Trace Element Iron Addition

Bianca Amartya Prabowo, Iqbal Syaichurrozi*, Achmad Faizal Ibrahim, Farhan Fadlurohman Tsaqif, Muhamad Ariel Satria, Muhammad Doni Fachriza, Alia Badra Pitaloka

Department of Chemical Engineering, Faculty of Engineering, Universitas Sultan Ageng Tirtayasa, Jl. Jendral Soedirman Km 3, Cilegon, 42435, Indonesia

ABSTRACT

The industries of tapioca starch processing result in a substantial amount of liquid waste (TSPW), characterized by high concentrations of organic compounds. Because of its chemical oxygen demand (COD), the tapioca wastewater is not permitted to be thrown away directly into the surrounding. The new method of combination of anaerobic digestion (AD) and microbial electrolysis cell (MEC) is proposed to be applied to convert COD in the tapioca wastewater to biogas. The main objective of this study is to examine the impact of $FeCl_3$ addition on MEC-AD performance in converting tapioca wastewater to biogas. The $FeCl_3$ dose varied to 0 (control), 200, 400, 600, and 800 mg/L. The results revealed that $FeCl_3$ doses of 0, 200, 400, 600, and 800 mg/L generated total biogas yields of 197.1, 276.11, 261.2, 239.48, and 202.2 mL/g-COD_{added}, respectively. Then, the $FeCl_3$ doses of 0, 200, 400, 600, and 800 mg/L achieved COD removals of 62, 71, 66, 65, and 63%, respectively. Furthermore, the $FeCl_3$ doses of 0, 200, 400, 600, and 800 mg/L had total solid (TS) removals of 33, 51, 48, 35, and 27%, respectively. Hence, the optimal $FeCl_3$ dose in MEC-AD of tapioca wastewater is 200 mg/L. Through the modified Gompertz model, the $FeCl_3$ dose of 200 mg/L had the highest P_m value (275.94 mL/g-COD_{added}) and the highest μ value (186.61 mL/g-COD_{added}/day).

Keywords: anaerobic digestion, biogas, microbial electrolysis cell, tapioca liquid waste.

1. INTRODUCTION

Tapioca starch, a polysaccharide derived from cassava roots (*Manihot esculenta*), is widely utilized in various industries, particularly food, pharmaceuticals, textiles, and adhesives. Its unique physicochemical properties, such as high viscosity and excellent binding capabilities, make it an essential ingredient across these sectors [1,2]. The substantial global production of tapioca starch is primarily concentrated in tropical regions, notably Southeast Asia, where it is integral to local economies and plays an important role in the supply chains globally [3]. However, the production and processing of this starch yield significant volumes of waste, both solid and liquid, raising serious environmental concerns regarding waste management [4].

Solid waste from the tapioca industry, predominantly composed of fibrous residues, presents opportunities for repurposing. These materials can be utilized as animal feed or soil conditioners, enhancing resource efficiency and minimizing landfill impact [3,4]. Conversely, the liquid waste generated, characterized by high organic content, poses serious environmental threats such as water pollution and eutrophication when inadequately treated [5]. The production of biogas from wastewater generated during tapioca processing has gained attention as an effective strategy to address these challenges [6].

One proven method for turning organic waste into biogas is anaerobic digestion (AD). Biogas is dominated by methane (CH_4) and carbon dioxide (CO_2) content, thereby

*Corresponding author:
E-mail: iqbal_syaichurrozi@untirta.ac.id (Iqbal Syaichurrozi)
How to cite: Prabowo, et al., Jurnal Teknik Kimia dan Lingkungan 10 (2026) 75–90.

Submitted : September 16, 2025
Revised : February 08, 2026
Accepted : February 25, 2026

offering a promising renewable energy source while simultaneously addressing waste management issues [7]. However, the efficiency of biogas production from starch-rich wastewater, such as that generated from tapioca processing, can often be hampered by nutrient imbalances and the accumulation of inhibitory by-products [8].

A significant strategy to enhance methanogenesis in these AD systems is the supplemental inclusion of trace elements, particularly iron (Fe). Iron serves as a critical cofactor for various enzymes essential for microbial metabolism and the methanogenic processes [9]. Research indicates that the addition of iron supplements can stabilize biogas outputs and enhance overall process performance during AD [10]. Specifically, iron is crucial for facilitating electron transfer, which is vital for microbial activity, especially in nutrient-scarce conditions that commonly characterize organic waste substrates [11].

Furthermore, integrating AD with microbial electrolysis cell (MEC) presents an innovative methodological advancement to improve biogas yields. MEC systems can introduce an external voltage that encourages microbial degradation of complex organic compounds, thereby significantly amplifying methane production [12]. The combined approach of AD and MEC technology (namely MEC-AD), augmented with trace element supplementation, presents a synergistic strategy to enhance energy recovery from high-strength organic waste, such as that produced during tapioca starch processing [13]. In particular, the incorporation of iron as a trace element has been effective in enhancing methane production within anaerobic digestion systems. Iron serves as a crucial cofactor for various enzymes involved in microbial metabolism and methanogenesis, which are essential for sustaining microbial activity in nutrient-limited conditions [14].

Several authors have examined biogas production from various wastes, a previous study [14] studied the utilization of tofu-processing wastewater (TPW) as a biogas feedstock through a combination of anaerobic digestion (AD) and anaerobic digestion assisted by microbial electrolysis cells (MEC-AD) with graphite electrodes at a voltage of 1.0 V and varying additions of $FeCl_3$ (0-600 mg/L) at pH 7.0. The results showed that MEC-AD increased biogas production by 14.4-114.5% compared to conventional AD, with optimal conditions at 400 mg-$FeCl_3$/L yielding 34.0 mL-CH_4/g-COD_{added}. MEC-AD also increased the efficiency of COD, TS, TSS, and TDS removal, which increased by 1.09, 1.26, 1.63, and 1.17 times, respectively, compared to AD, and produced 1.5 times higher energy surplus (5325.1 J) compared to AD (3582.1 J). A previous study [15] studied the treatment of tapioca wastewater into biogas through the AD and MEC-AD with graphite electrodes at a voltage of 1.0 V and the addition of urea in the range of 0-1.5 g. The results showed that MEC-AD without urea produced 2.3 times more biogas than AD, with a COD removal efficiency of 21% compared to 14%. With the addition of urea up to 1.5 g, biogas production increased from 106.4 to 268.9 mL/g-COD, while COD removal efficiency rose from 21% to 38%. A dose of 1.5 g produced the best performance because it was able to maintain pH stability and produce the highest VFA accumulation. A previous study [16] studied biohydrogen production from Palm Oil Mill Effluent (POME) using graphite electrodes at a fixed voltage of 1.0 V, with variations in initial pH (3.9, 6.0, 7.0) and two process schemes, namely dark fermentation (DF) only and single-stage DF + microbial electrolysis cell (sDFMEC). The best results were obtained with sDFMEC at pH 6.0, with cumulative hydrogen production reaching 83.39 mL-H_2/g-SCOD, final acetic acid accumulation of 10.658 mg-acetic acid/L with a production rate of 1.137 mg-acetic acid/L·day, compared to DF at pH 6.0, which produced 10.162 mg-acetic acid/L with a rate of 614 mg-acetic acid/L·day. The addition of MEC increased the recoverable energy surplus from 12.3 kJ (DF) to 25.8 kJ per liter of POME, which is an energy increase of approximately 2.1 times.

The aim of this current study on the influence of iron supplementation on biogas generation in an integrated MEC-AD system utilizing liquid waste from tapioca starch processing is particularly relevant, as a previous study [14] has demonstrated that trace element additives can lead to improvements in biogas yields. Specifically, the presence of iron facilitates electron transfer among microbial communities, thereby enhancing overall microbial efficiency and methane production. Research indicates that the inclusion of trace elements like iron can increase methane production volume in anaerobic systems processing organic waste [14].

Moreover, integrating MEC technology with AD allows for a more efficient conversion of substrates by applying an external voltage that stimulates microbial degradation and enhances the overall productivity of methanogenic organisms [17]. Thus, the objective to evaluate the influence of the addition of iron on biogas generation in an integrated MEC-AD system using liquid waste from tapioca starch processing is positioned to provide insights into optimizing trace element supplementation for improved biogas yield.

A previous study [14] investigating the $FeCl_3$ dose of 0-600 mg-$FeCl_3$/L or around 0-207 mg-Fe^{3+}/L in the AD and MEC-AD for biogas production from tofu wastewater. Then, a previous study [18] used doses of 156-390 mg-Fe^{3+}/L in AD of waste activated sludge. Therefore, in this study, the $FeCl_3$ addition was varied in the range of 0–800 mg/L or around 0-273.5 mg-Fe^{3+}/L. These values are in the range of doses used by the previous studies.

2. MATERIALS AND METHODS

2.1. Materials

The main substrate in the current research was tapioca starch processing wastewater (TSPW). The TSPW was taken from the settling stage of the home-scale tapioca flour manufacturing process. Before application, the substrate was homogenized to maintain consistency. The inoculum originated from fresh rumen fluid collected at a slaughterhouse in Jombang District, Cilegon City, Banten Province, Indonesia. Fresh rumen fluid was chosen because it contains abundant hydrolytic, acidogenic, acetogenic, and methanogenic microorganisms that are essential for the AD process. Detailed characteristics of TSPW and inoculum can be seen in Table 1.

The graphite plates (black, purity of 99.9%) were cut with dimensions of length× width×thickness of about 4.1×2.3×0.4 cm. Additionally, sodium hydroxide (NaOH) was used to regulate the pH, ensuring the initial pH was 7.0 for optimal microbial activity.

Table 1. Parameters of TSPW and inoculum.

Parameters	Units	TSPW	Inoculum
pH	-	4.03	4.2
Total COD	mg-O_2/L	5,207	20,635.83
VFAs	mg-acetic-acid/L	245.85	8,850.66
TS	mg-dry matter /L	12,500	46,500
TSS	mg-dry matter /L	8,250	15,000
TDS	mg-dry matter /L	4,250	31,500

Note: VFAs (volatile fatty acids), TS (total solid), TSS (total suspended solid), TDS (total dissolved solid).

2.2. Experimental Setup

The anaerobic batch digester was constructed using an erlenmeyer flask with a total volume of 600 mL. The reactor was operated in batch mode. During the process, the produced biogas was channeled through a saturated salt solution into a reversed measuring cylinder to quantify biogas volume. A liquid sampling port was placed at the base of the reactor. Graphite electrodes (black, 99.9% purity) served as both the anode and cathode, positioned around 1.1 cm apart. These electrodes were connected to the positive and negative terminals of a DC power supply (Long Wei, LW-K3010D series, 0-30 V, 0-10 A). A schematic illustration of the experimental setup is provided in Figure 1.

2.3. Experimental Design

The TSPW and inoculum were combined in a mixing tank at a volume ratio of 80:20 (v/v). The $FeCl_3$ dose was varied to 0, 200, 400, 600, and 800 mg/L. The initial pH was adjusted to 7.0. A detailed experimental design can be seen in Table 2.

2.4. Experimental Procedures

The substrate was prepared using a volumetric ratio of 80:20 (v/v) between total TSPW and inoculum with a total volume of 500 mL. $FeCl_3$ was added at varying concentrations (0-800 mg/L), and the pH was adjusted to 7.0 using 3 M NaOH. The entire mixture volume of 500 mL was loaded into the MEC-AD reactor. This working volume ensured that the electrodes (black graphite with 99.9% purity) were completely immersed, thus maintaining a constant surface area of the active electrodes (4.1×2.3×0.4 cm) in contact with the solution throughout the process. Anode and cathode were positioned at 1.1 cm. Anode and cathode were connected to a Long Wei LW-K3010D DC power supply (0-30 V, 0-10 A), with each electrode assigned to either the positive or negative pole. The process was conducted under ambient conditions (1 atm, 25-30 °C) with a constant applied voltage of 1.5 V.

Table 2. Design of experiments.

Trace element addition (mg $FeCl_3$/L)	TSPW volume (mL)	Inoculum volume (mL)	Initial pH
0	400	100	7.0
200	400	100	7.0
400	400	100	7.0
600	400	100	7.0
800	400	100	7.0

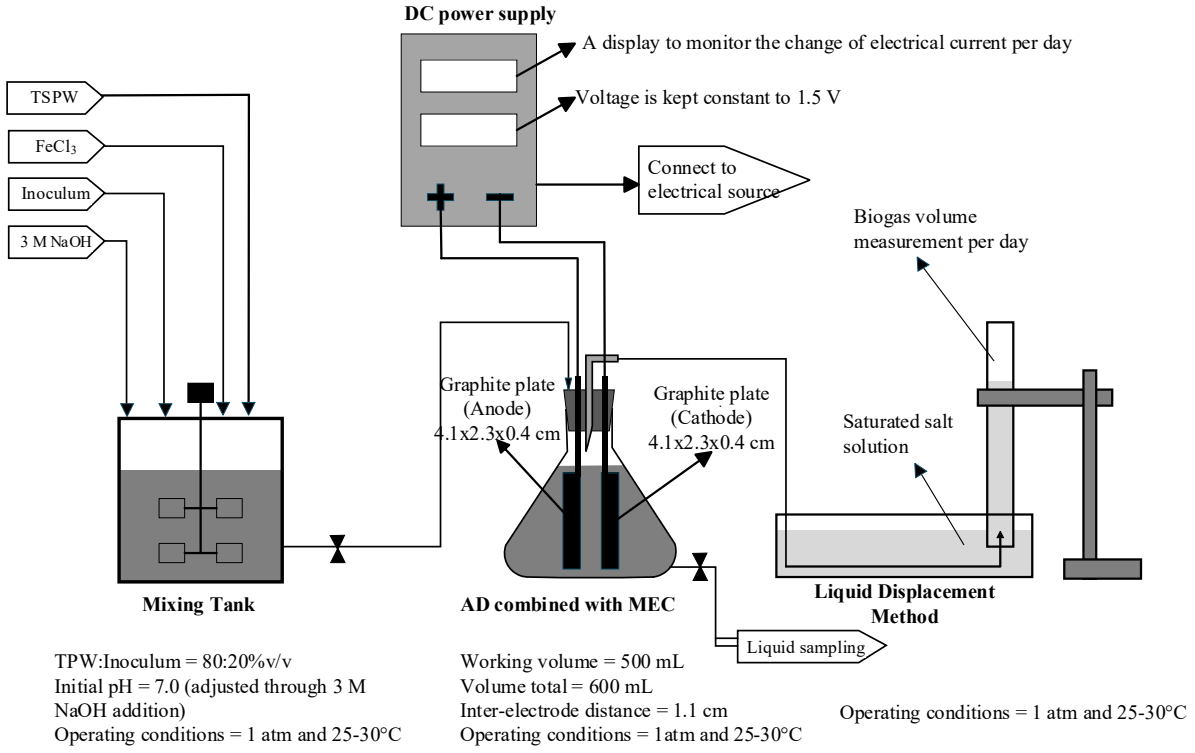

Figure 1. Lab-scale of MEC-AD technology.

The MEC-AD process was carried out until biogas production ceased completely. The biogas volume was quantified using the liquid displacement method. Additionally, every three days, liquid samples were collected from the digester base for monitoring of pH, COD, and VFAs.

2.5. Analysis

Approximately 10 mL of liquid samples were taken every three days. This process was carried out for 12 days. Liquid samples were obtained on days 3, 6, 9, and 12. The reduction in working volume was approximately 40 mL, or 8% of the total volume. This relatively small volume reduction kept the electrodes fully submerged, thus maintaining a constant surface area of the active electrode in contact with the solution throughout the process. Therefore, changes in working volume due to liquid sampling were negligible. In other words, the working volume was assumed to be constant.

2.5.1. Volatile Fatty Acid (VFA) Analysis

a. Preparation of Borax Solution

Disodium tetraborate heptahydrate ($Na_2B_4O_7 \cdot 10H_2O$) weighing 1.9079 g was dissolved in 100 mL of distilled water. The normality of the borax solution was calculated as 0.09955 N using Equation (1).

$$N_{borax} = \frac{\frac{Mass_{borax}}{MW_{borax}}}{Volume} \times purity \times equivalent\ valency \quad (1)$$

b. Standardization of 0.1 N H_2SO_4 Solution

Add 2-3 drops of methyl orange indicator to 5 mL of 0.1 N borax solution, then titrate with 0.1 N H_2SO_4 until the color changes from yellow to reddish orange. Normality of H_2SO_4 solution was quantified using Equation (2).

$$N_{H_2SO_4} = \frac{N_{borax} \times V_{borax}}{V_{H_2SO_4}} \quad (2)$$

c. Standardization of 0.05 N NaOH Solution

Add 2–3 drops of phenolphthalein indicator to 5 mL of 0.1 N H_2SO_4 solution, then titrate with 0.05 N NaOH until a stable pink color is formed. Normality of NaOH solution was quantified using Equation (3) and (4).

$$N_{NaOH} = \frac{N_{H_2SO_4} \times V_{H_2SO_4}}{V_{NaOH}} \quad (3)$$

The determination of the recovery factor commenced with the preparation of 2 mL of 0.7 N acetic acid solution, which was subsequently diluted with 50 mL of distilled water in a 250 mL Erlenmeyer flask. After that, add 2-3 drops of phenolphthalein indicator, then titrate the solution with 0.05 N NaOH until a stable pink endpoint is obtained, and record the volume of NaOH used as titrant volume 1 (V_1). For the distillation procedure, 2 mL of 0.7 N acetic acid was diluted to 100 mL using a measuring flask, then transferred to a 500 mL Erlenmeyer flask containing 100 mL of distilled water and 5 mL of 50% H_2SO_4. The distillation unit is then assembled with 600 W heating while maintaining a continuous flow of cooling water. The distillation process was carried out until 150 mL of distillate was obtained, which was then given 2–3 drops of phenolphthalein indicator and titrated with 0.05 N NaOH until a stable pink color was formed. The volume of NaOH used at this stage was recorded as titrant volume 2 (V_2). The recovery factor was calculated subsequently according to Equation (4).

$$F_{recovery} = \frac{V_2}{V_1} \quad (4)$$

d. VFA Analysis of the Sample

The concentration of VFA was determined based on the procedure reported by Syaichurrozi et al. [19,20] . A total of 2 mL of sample was pipetted into a 100 mL volumetric flask and diluted with distilled water to the mark. The solution was then transferred to a 500 mL erlenmeyer flask, 100 mL of distilled water and 5 mL of 50% H_2SO_4 were added, and then distilled using a 600 W hot plate until approximately 150 mL of distillate was collected. The distillate was given 2-3 drops of phenolphthalein indicator and then titrated with 0.05 N NaOH until a pink endpoint was reached. The VFA

analysis was then calculated using Equation (5).

$$VFAs\ \left(\frac{mg\ acetic\ acid}{L}\right) = \frac{V_{NaOH} \times N_{NaOH} \times MW_{acetic\ acid} \times 1000}{V_{sample} \times F\ recovery} \quad (5)$$

2.5.2. Chemical Oxygen Demand (COD) Analysis

The COD concentration was calculated using the method of Syaichurrozi et al. [19,20]. COD analysis was performed using the closed reflux method with spectrophotometry. The amount of 2 mL liquid sample was reacted with COD reagent in a vial, heated in a COD reactor at 150 °C for 2 hours, then cooled and measured with a COD meter. The COD of the sample is determined using Equation (6) where c is the COD reading on the COD meter and f is the dilution factor.

$$COD\ concentration\left(\frac{mg\ O_2}{L}\right) = \frac{C}{10} \times f \quad (6)$$

COD removal is obtained from the difference in influent COD and effluent COD values, which is calculated using Equation (7). It shows the level of decrease in organic material concentration during the anaerobic digestion process.

$$COD\ removal = \frac{COD_{influent} - COD_{effluent}}{COD_{influent}} \times 100\% \quad (7)$$

2.5.3. Total Solids (TS) Analysis

The TS content was calculated by following the procedure of Syaichurrozi et al. [20]. An oven-dried crucible was initially weighed (w_1). Next, a 10 mL sample was introduced into the crucible. The crucible filled by the sample was heated at 105°C until reaching a constant weight, cooled in a desiccator for 5 minutes, and then reweighed to obtain w_2. The TS concentration was calculated using Equation (8).

$$TS\left(\frac{mg}{L}\right) = \frac{w_2 - w_1}{V_{sample}} \quad (8)$$

2.5.4. Total Suspended Solids (TSS) and Total Dissolved Solids (TDS)

Filter paper (Whatman No. 42) was pre-dried in an oven and weighed (w_1). A 20 mL sample was filtered, and the filter paper containing wet solids was oven-dried at 105 °C until reaching constant weight, then reweighed (W_2). The values of TSS and TDS were subsequently calculated using Equation (9) and (10).

$$TSS\ \left(\frac{mg}{L}\right) = \frac{w_2 - w_1}{V_{sample}} \quad (9)$$

$$TDS = TS - TSS \quad (10)$$

2.5.5. pH Analysis

The pH of the liquid was determined using a digital pH meter (pH-009) on day 0 and subsequently every three days until biogas production was no longer observed.

2.5.6. Biogas Generation Analysis

Biogas generation was quantified through the liquid displacement method as described by Syaichurrozi et al. [20]. Biogas yield (mL/g-COD_{added}) was calculated by dividing the biogas volume by the initial COD of TSPW.

2.6. Kinetics

In the current research, the authors employed the modified Gompertz kinetic model. The kinetic model has three kinetic constants, namely P_m, μ, and λ (see Equation (11)). The kinetic model assumes that in the batch mode, the biogas generation profile follows the bacterial-specific growth profile. The Sum of Squared Error (SSE) was employed as an objective function, and the optimization was conducted using the tool of Microsoft Excel. The equation of SSE is shown in Equation (12).

$$P_t = P_m . exp\left\{-exp\left[\frac{\mu . e}{P_m}(\lambda - t) + 1\right]\right\} \quad (11)$$

$$SSE = \sum_{t=1}^{n}\left(P_i - \hat{P}_i\right)^2 \quad (12)$$

Where P_t is cumulative of biogas yield at time t (mL/g-COD_{added}), P_m is the maximum biogas yield that can be achieved (mL/g-COD_{added}), μ is maximum biogas production rate (mL/g-COD_{added}/day), λ is lag time (days), e is 2.718282, t is the operating time (days), P_i is the experimental biogas yield, and $\hat{P}_i$ is the modeled biogas yield.

3. RESULTS AND DISCUSSION

3.1. Biogas Production

Figure 2 illustrates the progression of biogas production during the MEC-AD processes namely the daily and cumulative biogas yield profiles observed throughout the research. The daily biogas production pattern depicted in Figure 2(a) demonstrates fluctuations in yield across all treatment variations. The most productive phase occurred between days 1 until 4, with a dose of 200 mg-$FeCl_3$/L reaching the peak yield of 126.52 mL/g-COD_{added} on day 1, and a dose of 400 mg-$FeCl_3$/L reaching the peak yield of 136.70 mL/g-COD_{added} on day 1. However, a noticeable decrease in daily biogas production was observed in all variations between days 5 and 12. The experimental pattern observed in MEC-AD systems is a rapid early peak in daily biogas production (commonly within the first 24-48 hours).

Figure 2(b) illustrates the cumulative biogas production. The highest total biogas yield for the MEC-AD system was at a dose of 200 mg-$FeCl_3$/L with 276.11 mL/g-COD_{added}, followed by a dose of 400 mg-$FeCl_3$/L with 261.2 mL/g-COD_{added}.

Microbial electrolysis cell-assisted anaerobic digestion (MEC-AD) integrates the electrochemical cell within an anaerobic digester to supply an extracellular electron pathway that complements the conventional four stages of AD (hydrolysis, acidogenesis, acetogenesis, methanogenesis). The imposed electrochemical conditions and electrode surfaces enrich exoelectrogenic bacteria at the anode, which oxidize VFAs and labile organics to H^+, CO_2, e^-, as described in Equation (13) [14].

$$CH_3COOH + 2H_2O \rightarrow 2CO_2 + 8H^+ + 8e^- \quad (13)$$

Then, these products are subsequently consumed by hydrogenotrophic methanogens to reduce H^+, CO_2, and e^- to CH_4 at the cathode via direct interspecies electron transfer (DIET)-based methanogenesis as described in Equation (14) [14].

$$CO_2 + 8H^+ + 8e^- \rightarrow CH_4 + 2H_2O \quad (14)$$

During MEC-AD, hydrogenotrophic methanogens are more dominant at cathode than acetoclassical methanogens. Then, acetoclassical methanogens are more dominant in the bulk solution than hydrogenotrophic. Hence, in the bulk solution, the methane can be formed through indirect interspecies electron transfer (IIET)-based methanogenesis, namely acetoclastic methanogenesis (Equation (15)) and hydrogenotrophic methanogenesis (Equation (16)) [21].

$$CH_3COOH \rightarrow CH_4 + CO_2 \quad (15)$$

$$CO_2 + 4H_2 \rightarrow CH_4 + 2H_2O \quad (16)$$

In this study, the $FeCl_3$ was added as a trace element. The results showed that the optimal dose was 200 mg-$FeCl_3$/L. Iron (Fe) is a vital trace element for anaerobic microorganisms, making up around 0.07-0.28% of the biomass of methanogenic cells [22]. Iron supplied as $FeCl_3$ performs multiple complementary functions. It serves as an essential micronutrient and cofactor for redox enzymes central to methanogenesis, it modifies particle/colloid surface chemistry, thereby affecting hydrolysis and mass transfer, and it can participate in Fe(III)/Fe(II) redox cycling that facilitates electron flow in the mixed matrix [23,24]. Appropriate Fe dosing enhances enzyme activity and promotes an increase in both hydrolytic microorganisms and exoelectrogens, which accelerates consumption of labile COD and amplifies early biogas production. Conversely, excessive Fe dosing can reduce performance by precipitating organics/inorganics, altering substrate bioavailability, or forming strong complexes with protein functional groups that perturb enzyme structure and function [25].

The presence of iron influence the process via two ways, namely biologically and chemically. In biologically way, the iron is a key component of methanogenic enzymes and a redox cofactor for methyl-coenzyme M (CoM), so increasing Fe concentrations can enhance enzyme function, increasing the conversion of acetic acid to methane. Then,

in chemically way, Fe^{2+} can form $Fe(OH)_2$ precipitates and complex compounds that are more easily precipitated and can bind acetic acid. The Fe^{2+} can react with acetic acid to form precipitate (Equation (17)).

$$Fe^{2+} + 2CH_3COO^- \leftrightarrow Fe(CH_3COO)_2 \quad (17)$$

Because of its irreversible reaction, the precipitate can release the acetic acid into the liquid (Equation (18)). Therefore, the microbes then convert the acetic acid back into higher biogas production and increase COD and TS removal [26].

$$Fe(CH_3COO)_2+H_2O\leftrightarrow Fe(OH)(CH_3COO)\downarrow+CH_3COOH \quad (18)$$

Based on Figure 2(c), the average of electrical current at a dose of 200 mg-$FeCl_3$/L was higher than that at the control (0 mg-$FeCl_3$/L). It means that the addition of $FeCl_3$ increased the conductivity and the electrical current, so increased the activity of exoelectrogenic bacteria. However, when the $FeCl_3$ dose was increased to 400-800 mg-$FeCl_3$/L, the excess Fe formed more deposits and flocs that accumulated inside the digester and on the electrode surface. These deposits increased electrical resistance and decreased the electrical current. Figure 2(c) shows that the electrical current at doses of 400-800 mg-$FeCl_3$/L was lower than that at a dose of 200 mg-$FeCl_3$/L. Because the voltage is kept constant (V = I.R), the increased resistance results in a lower current, which reduces the electron flux to the cathode and weakens DIET-based methanogenesis. Consequently, methane production and treatment performance decrease at higher Fe concentrations (400-800 mg-$FeCl_3$/L).

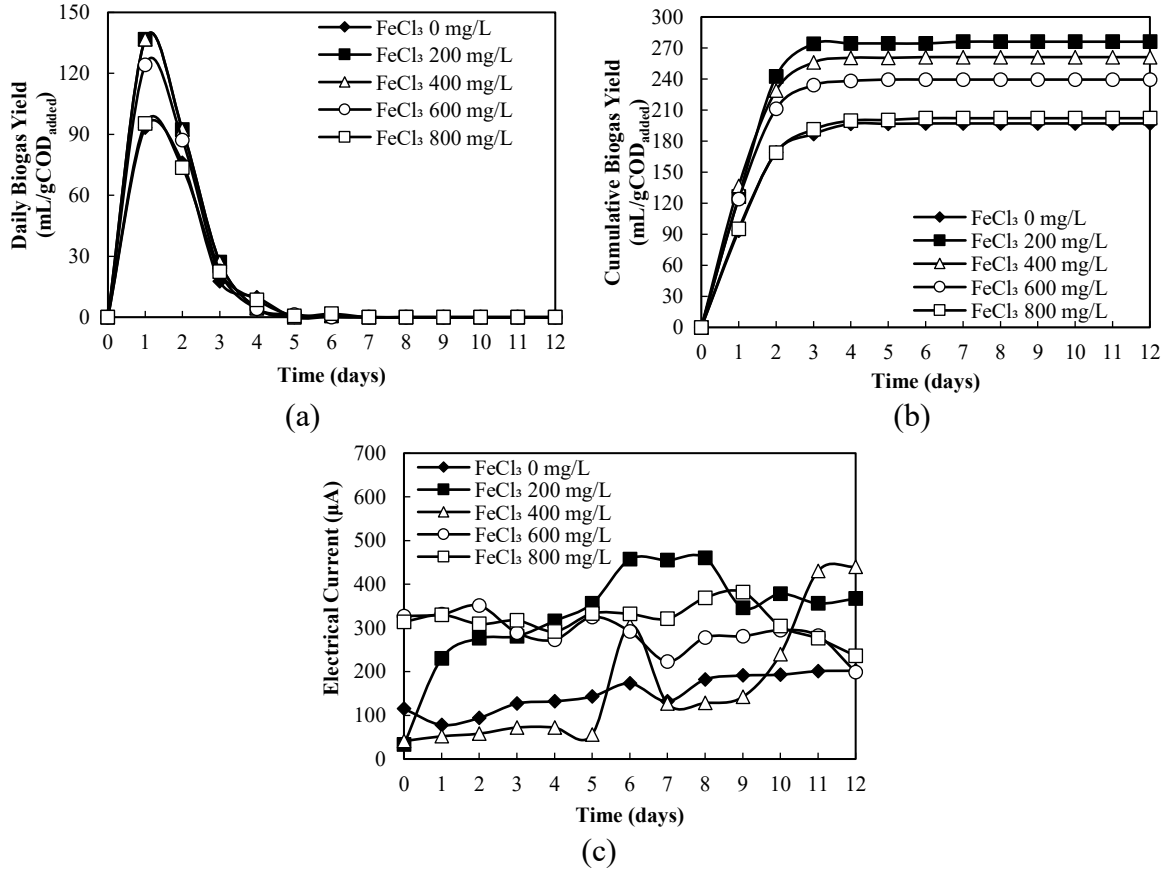

Figure 2. Variation of initial pH to (a) daily biogas yield, (b) cumulative biogas yield, (c) electrical current.

Figure 2(c) show that the 200 mg-$FeCl_3$/L exhibits the highest average current (331.6 µA) and achieved high peaks (up to 460 µA) indicate strong electron flux and likely enrichment/activation of electroactive microbes. Such electroactivity is a necessary condition for MEC-enhanced hydrogen/methane production. The increased

early-stage hydrogen and methane production is because hydrogenotrophic methanogens or DIET pathways are active [27,28].

In this study, the optimal Fe dose in MEC-AD of TSPW was 200 mg-$FeCl_3$/L is equal to around 67 mg-Fe^{3+}/L. A previous study [18] found the different optimal dose, namely 234 mg-Fe^{3+}/L, in the AD of waste activated sludge. Then, a previous study [29] found the different optimal dose, namely 290 mg-Fe^{3+}/L, in the AD of vinasse. The different findings between this study and previous studies might be caused by the characteristics of substrates and inoculums, the form of Fe sources, and the process (AD or MEC-AD).

3.2. pH and VFAs

pH plays a crucial role in anaerobic digestion process, as it significantly influences microbial growth. The pH inside the digester is largely determined by the levels of VFAs and ammonia/ammonium formed along the process. To ensure effective microbial performance, the pH must be maintained within the optimal range of 6.5 to 8.2 [30]. Figure 3(a) shows the pH trend for each treatment over a 12-day period. At the beginning of the process, all digesters had an initial pH of 7.0. As shown in Figure 3(a), the pH values in the MEC-AD process with Fe doses of 0 mg-$FeCl_3$/L, 200 mg-$FeCl_3$/L, 400 mg-$FeCl_3$/L, 600 mg-$FeCl_3$/L, and 800 mg-$FeCl_3$/L decreased to 6.41, 6.44, 6.48, 6.48, and 6.49 on day 12, respectively. This decrease in pH was due to the accumulation of VFAs.

The observed decrease in pH indicates that acidogenesis is taking place in the digester. The MEC-AD, augmented with $FeCl_3$, simultaneously accelerates hydrolysis and acidogenesis by providing alternative electron acceptors via dissimilatory iron reduction (DIR) and alters the chemical fate of produced VFAs through Fe^{2+}/$Fe(OH)_2$, mediated adsorption or precipitation. As a result, Fe addition changes both the magnitude and timing of VFA accumulation and the concomitant pH response [18]. In Figure 3(a) it can be seen that all digesters started at pH 7.00 and experienced the lowest pH on day 3, namely 6.17, 6.26, 6.24, 6.18, and 6.27 for 0, 200, 400, 600, and 800 mg-$FeCl_3$/L, consistent with a rapid acidification phase as hydrolysis produces VFAs faster than methanogens can consume them and the individual VFA concentrations were ranked as follows: acetic acid then butyric acid then propionic acid [24]. The VFA time series show a clear universal peak on day 3 for every dose (namely 3,028.28, 2,704.37, 2,851.88, 2,901.05, and 2,610.59 mg-acetic acid/L for doses of 0, 200, 400, 600, and 800 mg-$FeCl_3$/L), which indicates that Fe addition in this tests tended to reduce the measured soluble VFA peak relative to the control, rather than increasing it beyond the control peak [26]. Mechanistically, DIR and Fe-mediated enzyme effects explain that Fe(III) can stimulate hydrolysis/acidogenesis so more VFA is produced biologically while subsequent formation of Fe(II) complexes or $Fe(OH)_2$(s) can transiently remove acetate from the dissolved phase, so the measured soluble VFA peak and the pH minimum reflect the net balance between production, biological consumption (methanogenesis), and Fe-mediated chemical sequestration [18,29].

VFAs are the primary acidification products (substrates for methanogenesis), so an early rapid VFA rise causes the observed pH fall, and when methanogens or other consumers subsequently degrade VFAs [31]. Figure 3(b) shows that the day-3 VFA maximum coincides with the acidogenesis peak when hydrolysis of TSPW is fast and rumen inoculum is highly active, while the reported highest daily biogas occurs slightly earlier (day 2) because early fermentative pathways can produce gas quickly before VFA reaches its maximal soluble concentration. This sequencing (biogas rate peak preceding or near VFA peak) is consistent with MEC-AD and pretreated sewage sludge studies, where VFAs accumulate rapidly after 48-72 h and then are consumed by methanogens [31,32].

Thermophilic investigations have reported inhibition thresholds on the order of several grams per litre. A critical total VFA (TVFA)

concentration near 6,900 mg/L has been reported in thermophilic $FeCl_3$ studies. The highest TVFA measured in Figure 3(b) (at a dose 0 mg-$FeCl_3$/L with 3,028.28 mg-acetic acid/L) is substantially below that reported thermophilic inhibition threshold, which indicates that observed VFA accumulation likely caused reversible acid stress rather than irreversible collapse of the methanogenic community [24].

In Figure 3(b), it is shown that control (0 mg-$FeCl_3$/L) produced the largest soluble VFA peak, whereas intermediate Fe additions (200-400 mg-$FeCl_3$/L) commonly offer the best compromise between accelerated hydrolysis and controlled VFA accumulation, resulting in improved methane yields. Mechanistically, moderate Fe dosing supplies essential enzymatic cofactors and promotes Fe-assisted routing of acetate into methanogenesis, while permitting reversible sequestration of acetate without imposing severe enzyme inhibition or electron-competition that would suppress methanogens [23].

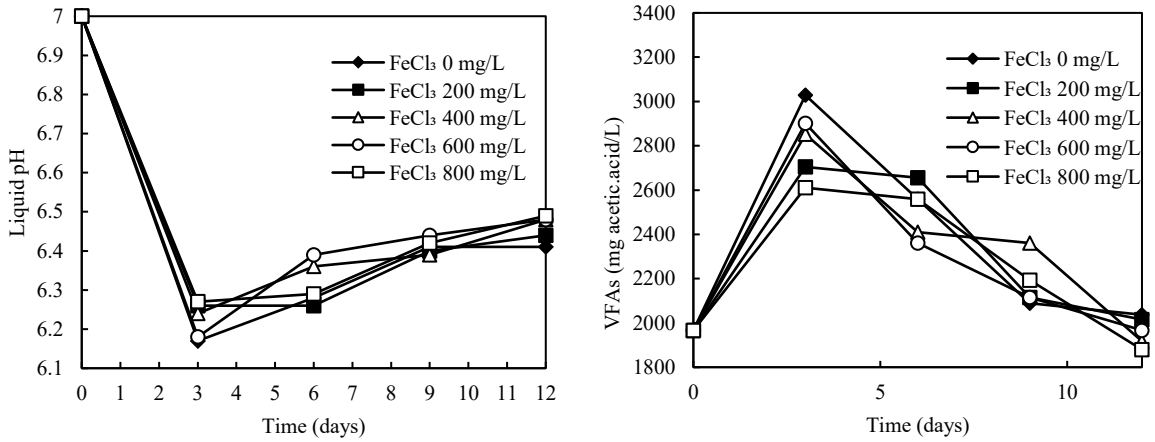

Figure 3. Production of (a) pH Liquid, (b) volatile fatty acids (VFAs).

The addition of $FeCl_3$ affected the dynamics of volatile fatty acids and pH during the MEC-AD process. At medium $FeCl_3$ doses, VFAs consumption was more stable, so the system pH remained within a range that supported the activity of methanogenic microorganisms. This indicates that Fe plays a role in accelerating VFAs conversion during the methanogenesis stage. Conversely, at higher $FeCl_3$ doses, VFAs accumulation and greater pH fluctuations indicated a disruption in the balance between acidogenesis and methanogenesis, which negatively impacted process stability and biogas production.

3.3. TS, TSS, TDS, and COD Removal

MEC-AD biogas can be produced not only through DIET-based methanogenesis but also through IIET-based methanogenesis [28]. Additionally, there is a necessity to supplement trace elements to maintain process stability in mesophilic biogas production. The supplementation of trace elements can become essential to sustain methanogenic activity and to get high organic loading rates (OLRs), which are critical for maximizing methane yield and process efficiency [33]. Thus, the incorporation of MEC together with trace elements can enhance biogas production and improve the removal efficiencies of COD, TS, TSS, and TDS, which displayed a clear dependence on $FeCl_3$ concentration, and these variations were strongly reflected in the cumulative yield of biogas production.

Figures 4(a), 4(b), 4(c), and 4(d) show the removals of COD, TS, TSS, and TDS, respectively. At the baseline without $FeCl_3$ addition, the system achieved a COD removal of 62%, TS removal of 33%, TSS removal of 22%, and TDS removal of 43%,

resulting in a cumulative methane yield of 197 mL/gCOD$_{added}$. Supplementation with 200 mg-$FeCl_3$/L produced the highest performance, achieving COD removal of 71%, TS removal of 51%, TSS removal of 19%, and TDS removal of 82%. This condition also yielded the maximum cumulative methane production of 276 mL/gCOD$_{added}$, confirming the critical role of $FeCl_3$ in enhancing enzymatic activity, promoting electron transfer, and stabilizing mesophilic and methanogenic populations.

When the $FeCl_3$ dose was further increased to 400 mg-$FeCl_3$/L, COD removal decreased slightly to 66% and TDS removal to 66%, with methane yield declining to 261 mL/gCOD$_{added}$. At 600 mg-$FeCl_3$/L, COD removal was recorded at 65% and TDS removal at 59%, resulting in a methane yield of 239 mL/gCOD$_{added}$. The poorest performance occurred at 800 mg-$FeCl_3$/L, with COD removal of 63%, TS removal of 27%, TSS removal of 17%, and TDS removal of 38%, accompanied by the lowest methane yield of 202 mL/gCOD$_{added}$. As a result, the system exhibited faster stabilization of biogas production within the first four days, particularly at 200 mg-$FeCl_3$/L, where the highest methane yield was recorded. The synergistic effect between $FeCl_3$ supplementation and MEC operation confirmed that 200 mg/L $FeCl_3$ provided the optimum condition.

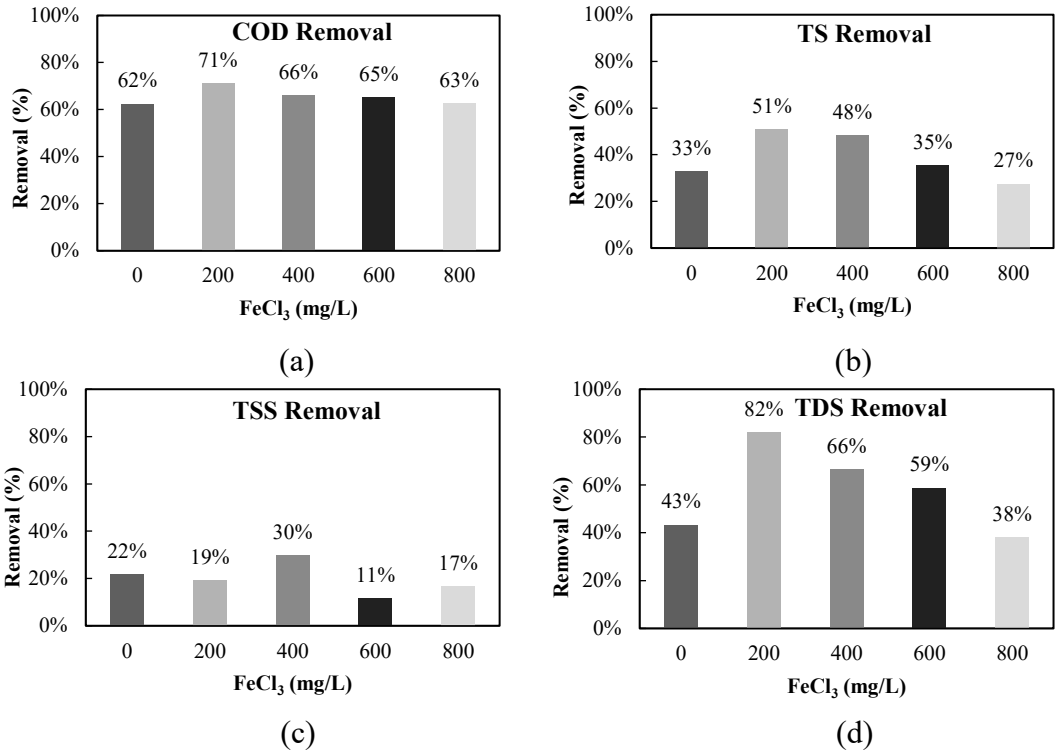

Figure 4. Organic and solid removal efficiency; (a) COD removal; (b) TS removal; (c) TSS removal; (d) TDS removal.

The overall trend demonstrates that methane yield was closely aligned with COD removal. The correlation between total biogas yield and COD removal efficiency shows good linier correlation with an equation of COD removal = 0.0932×total biogas yield+43.615 with R^2 of 0.8501 (Figure 5). However, it still shows that improvements in COD removal do not always correspond to increased biogas production. According to Syaichurrozi et al. [19], the COD removal was not only for methane production, but also for the generation of intermediate products and the consumption for microbial growth and maintenance.

During the MEC-AD with the presence of $FeCl_3$, there is not only electrobiochemical mechanisms but also physicochemical

mechanisms such as precipitation and adsorption of organic compounds by Fe^{3+} or $Fe(OH)_3$. If the effluent of the MEC-AD reactor was settled, the resulting supernatant might contain lower COD values. However, in this experiment, before liquid sampling, the liquid in the reactor was homogenized, so the COD removal due to precipitation cannot be seen.

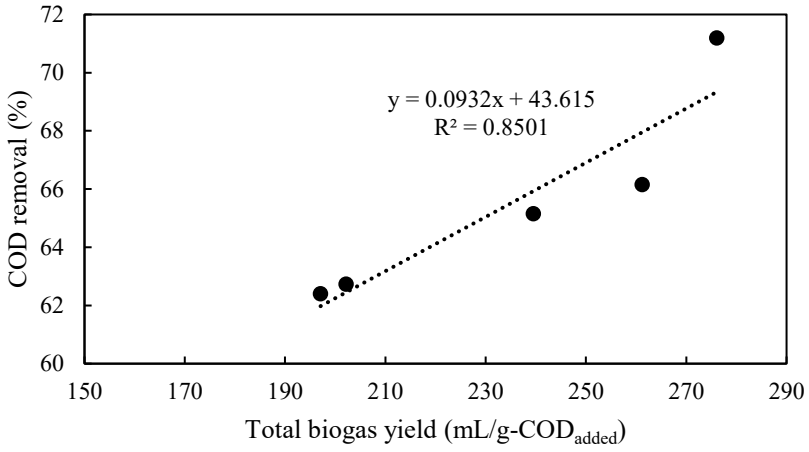

Figure 5. Correlation between total biogas yield and COD removal.

3.4. Kinetic Analysis

The plotting of modeled data on the experimental data is shown in Figure 6. The values of P_m, μ, and λ are shown in Table 3. $FeCl_3$ doses of 0, 200, 400, 600, and 800 mg/L had P_m values of 196.97, 275.94, 261.31, 239.49, and 201.95 mL/g-COD_{added}, respectively. Thus, the $FeCl_3$ dose of 200 mg/L was the optimum dose because this dose can produce the highest biogas yield. The μ shows the rate of biogas formation. The value of μ increases with an increase in P_m, indicating that the potential biogas yield will increase in line with the increasing rate of biogas formation, as reported in previous studies [34]. The addition of 200 mg/L $FeCl_3$ produced the highest P_m and μ values (Table 3), so this dose was able to increase microbial activity while accelerating the rate of biogas formation. Meanwhile, λ is the adaptation time required by anaerobic microbes before they start producing biogas [35,36] with a $FeCl_3$ dose of 200 mg/L also gave the highest λ value, which was 0.32 days.

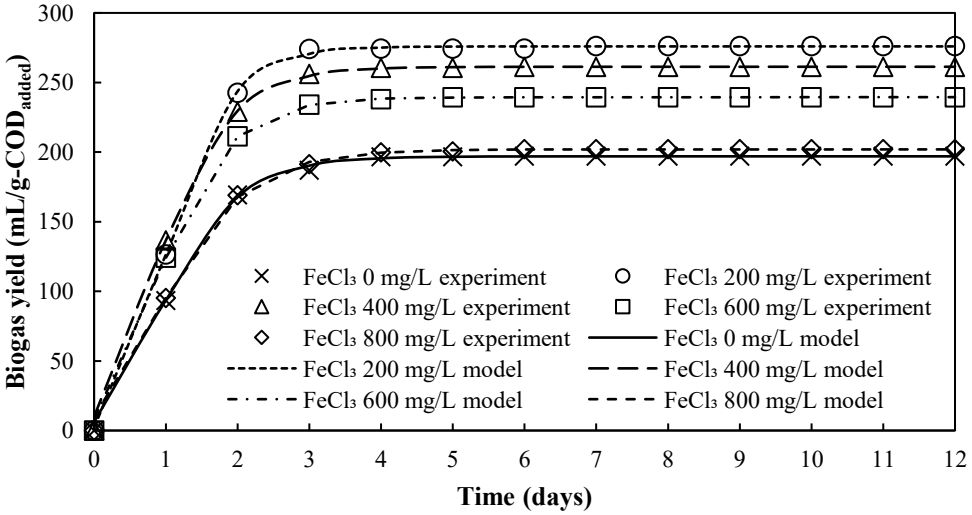

Figure 6. Plotting results using the modified Gompertz model.

Table 3. Kinetic constant values.

Constants	Units	$FeCl_3$ addition (mg/L)				
		0	**200**	**400**	**600**	**800**
P_m	mL/g-COD_{added}	196.97	275.94	261.32	239.49	201.95
μ	mL/g-COD_{added}/day	111.33	186.61	155.13	146.28	104.09
λ	days	0.16	0.32	0.11	0.14	0.08
P_m experiment	mL/g-COD_{added}	197.1	276.1	261.2	239.5	202.2
Error	%	0.06	0.06	0.05	0.01	0.11

Based on the kinetic analysis using the modified Gompertz model, a dose of 200 mg-$FeCl_3$/L resulted the highest biogas potential (P_m) of 275.94 mL/g-COD_{added}. This value is almost same as the experimental total biogas yield which was 276.1 mL/g-COD_{added}. It means that the modified Gompertz model can predict the total biogas yield accurately with an error of 0.06%.

3.5. Challenges in Implementation

Currently, this research was conducted at a laboratory scale using Erlenmeyer flasks, allowing for tight control of variables but did not fully represent industrial-scale operational conditions. This laboratory scale experiment shows that the MEC-AD with the $FeCl_3$ addition successfully enhance conversion of TSPW to biogas. However, operational challenges at an industrial scale include electrode selection, electrode maintenance, controlling the $FeCl_3$ dose, and managing solids accumulation, which can affect system stability. At an industrial scale, MEC-AD implementation will face higher investment costs for infrastructure, as well as operational costs related to $FeCl_3$ use and sludge management. However, the potential for energy recovery from biogas could help offset some of these costs. To confirm its economic feasibility, further pilot-scale studies and a more in-depth cost analysis are needed.

3.6. Limitations and Future Research

This research revealed that the optimal dose for producing biogas from TSPW via MEC-AD was 200 mg-$FeCl_3$/L. However, there are several limitations in this research. This research only focused on the effect of $FeCl_3$ addition in the MEC-AD process. The $FeCl_3$ addition in the AD without MEC was not carried out. It is because this research is a continuation of previous research [15]. In the previous study [15], the MEC-AD generated a higher biogas yield than the AD at various urea additions. Therefore, in this study, the authors only focused on the MEC-AD. However, the comparison between MEC-AD and AD should be conducted with the optimal $FeCl_3$ dose in the two process to ensure the superiority of the MEC-AD.

The experiment in this research was conducted in a short-term batch mode until biogas production ceased which is 12 days, indicating the initial digestion phase rather than the long-scale continuous operation performance. Consequently, the results may not fully represent the steady-state behavior or robustness of the MEC-AD system under practical, large-scale conditions. A detailed microbial community analysis was not performed. Therefore, the roles of exoelectrogens, hydrogenotrophic methanogens, and acetoclastic methanogens were inferred indirectly from process indicators such as biogas yield, COD removal, and current profiles. If the information of the changes in microbial communities is available, the mechanism reactions during MEC-AD with the presence of $FeCl_3$ can be predicted accurately. Key electrochemical parameters such as electrode potential, internal resistance, and electron transfer efficiency were not directly measured, limiting the quantitative understanding of how $FeCl_3$ addition affects electron flux and the DIET mechanism.

Therefore, future studies should focus on long-term continuous or semi-continuous

operation, microbial community characterization, and detailed electrochemical analysis of trace metal elements and electron transfer pathways to enable more reliable scaling and optimization of the MEC-AD system. Additionally, the research on the impact of $FeCl_3$ addition with a narrower variation in Fe doses (0-200 mg-$FeCl_3$/L) to ensure that the most optimal dose is 200 mg-$FeCl_3$/L needs to be conducted in the future.

4. CONCLUSION

This study demonstrated that the $FeCl_3$ addition strongly influences the MEC-AD performance of tapioca wastewater. Among the tested conditions, the $FeCl_3$ addition of 200 mg/L achieved the highest biogas yield (276.1 mL/g-COD_{added}), the greatest COD (71%) and TS (51%) removals, and the most favorable kinetic parameters according to the modified Gompertz model (P_m = 275.94 mL/g-COD_{added}; μ = 186.61 mL/g-COD_{added}/day). These findings indicate that the $FeCl_3$ addition of 200 mg/L optimizes microbial activity and maximizes biogas production. Therefore, the $FeCl_3$ dose of 200 mg/L is recommended as the optimal condition for efficient MEC-AD of tapioca wastewater.

ACKNOWLEDGMENT

The authors would like to thank the "Direktorat Penelitian dan Pengabdian kepada Masyarakat (DPPM), Direktorat Jenderal Riset dan Pengembangan, Kementerian Pendidikan Tinggi, Sains dan Teknologi-Indonesia" for financial support through the Research Grant of "Penelitian Pasca Sarjana-Penelitian Tesis Magister 2025" with contract numbers 111/C3/DT.05.00/PL/2025 and B/625/UN43.9/PT.00.03/2025 and "Universitas Sultan Ageng Tirtayasa (Untirta) Indonesia" for laboratory facility support.

REFERENCES

1. J. Babić, D. Šubarić, D. Ackar, V. Piližota, M. Kopjar, N.N. Tiban, Effects of pectin and carrageenan on thermophysical and rheological properties of tapioca starch, Czech Journal of Food Sciences 24 (2006) 275–282.
2. Y. Kim, S.H. Yoo, K.H. Park, J.H. Shim, S. Lee, Functional characterization of native starches through thermal and rheological analysis, Journal of the Korean Society for Applied Biological Chemistry 55 (2012) 413–416.
3. W.S. Aji, P. Purwanto, S. Suherman, Good housekeeping implementation for improving efficiency in cassava starch industry (case study: Margoyoso district, Pati regency), E3S Web of Conferences 31 (2018) 05011.
4. J. Jerry, P. Febriyanto, A.W. Satria, Analysis of tapioca industrial solid waste as coal substitution, IOP Conference Series: Earth and Environmental Science 1209 (2023) 012012.
5. D.O. Prastiwi, N. Anggita, Y.P. Arishandy, Bioethanol production from tapioca-waste as potential additive fuel for LCGC (low-cost green car), Current Biochemistry 6 (2019) 28–34.
6. M.O. Fatehah, S. Hossain, T.T. Teng, Semiconductor wastewater treatment using tapioca starch as a natural coagulant, Journal of Water Resource and Protection 5 (2013) 1018–1026.
7. E.A. Economou, G. Dimitropoulou, N. Prokopidou, I. Dalla, T. Sfetsas, Anaerobic digestion remediation in three full-scale biogas plants through supplement additions, Methane 2 (2023) 265–278.
8. V. Chubur, D. Danylov, Y. Chernysh, L. Plyatsuk, V. Shtepa, N. Haneklaus, H. Roubik, Methods for intensifying biogas production from waste: A scientometric review of cavitation and electrolysis treatments, Fermentation 8 (2022) 570.
9. A.B.T. Nelabhotla, C. Dinamarca, Bioelectrochemical CO_2 reduction to methane: MES integration in biogas

production processes, Applied Sciences (Switzerland) 9 (2019) 1056.
10. N.I. Madondo, E.K. Tetteh, S. Rathilal, B.F. Bakare, Synergistic effect of magnetite and bioelectrochemical systems on anaerobic digestion, Bioengineering 8 (2021) 198.
11. W. Liu, W. Cai, Z. Guo, L. Wang, C. Yang, C. Varrone, A. Wang, Microbial electrolysis contribution to anaerobic digestion of waste activated sludge, leading to accelerated methane production, Renewable Energy 91 (2016) 334–339.
12. T. Bo, X. Zhu, L. Zhang, Y. Tao, X. He, D. Li, Z. Yan, A new upgraded biogas production process: Coupling microbial electrolysis cell and anaerobic digestion in single-chamber, barrel-shape stainless steel reactor, Electrochemistry Communications 45 (2014) 67–70.
13. K.R. Kunzler, S.D. Gomes, P.A. Piana, D.G.B. Torres, M.A.V. Boas, M.H.F. Tavares, Anaerobic reactors with biofilter and different diameter-length ratios in cassava starch industry wastewater treatment, Engenharia Agricola 33 (2013) 612–624.
14. I. Syaichurrozi, I. Murtiningsih, E.C. Angelica, D.Y. Susanti, J. Raharjo, G.E. Timuda, N. Darsono, S. Primeia, E. Suwandi, Kurniawan, D.S. Khaerudini, A preliminary study: Microbial electrolysis cell assisted anaerobic digestion for biogas production from Indonesian tofu-processing wastewater at various Fe additions, Renewable Energy 234 (2024) 121203.
15. N. Khomariah, I. Syaichurrozi, T. Kurniawan, Enhanced biogas production from tapioca wastewater through the microbial electrolysis cell-assisted anaerobic digestion process at various urea additions, Jurnal Bahan Alam Terbarukan 13 (2024) 146–155.
16. I. Syaichurrozi, M.A. Hidayatullah, A. Nurullah, E. Suhendi, I. Kustiningsih, D.Y. Susanti, N. Darsono, S. Primeia, D.S. Khaerudini, Enhanced biohydrogen production from palm oil mill effluent using single-stage process of dark fermentation and microbial electrolysis cell at various initial pHs, Renewable Energy 249 (2025) 123161.
17. J.R. Asztalos, Y. Kim, Lab-scale experiment and model study on enhanced digestion of wastewater sludge using bioelectrochemical systems, Journal of Environmental Informatics 29 (2017) 98–108.
18. W. Zhan, Y. Tian, J. Zhang, W. Zuo, L. Li, Y. Jin, Y. Lei, A. Xie, X. Zhang, Mechanistic insights into the roles of ferric chloride on methane production in anaerobic digestion of waste activated sludge, Journal of Cleaner Production 296 (2021) 126527.
19. I. Syaichurrozi, E. Suhendi, I. Kustiningsih, S. Nurulshani, A.A. Pramudita, N. Darsono, D.S. Khaerudini, Enhancement of biogas production through anaerobic co-digestion of tofu wastewater and cassava starch wastewater in Indonesia, Bioresource Technology Reports 33 (2026) 102557.
20. I. Syaichurrozi, A.F. Ibrahim, F.F. Tsaqif, E. Suhendi, I. Kustiningsih, H. Hashim, M. Hidayat, Biogas generation from liquid waste of Beneng taro starch processing : The effect of initial pH, Journal of Ecological Engineering 27 (2026) 55–68.
21. A. Hassanein, F. Witarsa, S. Lansing, L. Qiu, Y. Liang, Bio-electrochemical enhancement of hydrogen and methane production in a combined anaerobic digester (AD) and microbial electrolysis cell (MEC) from dairy manure, Sustainability (Switzerland) 12 (2020) 8491.
22. P. Scherer, H. Lippert, G. Wolff, Composition of the major elements and trace elements of 10 methanogenic bacteria determined by inductively coupled plasma emission spectrometry, Biological Trace Element Research 5 (1983) 149–163.
23. X. Hao, J. Wei, M.C.M. van Loosdrecht, D. Cao, Analysing the

mechanisms of sludge digestion enhanced by iron, Water Research 117 (2017) 58–67.
24. B. Yu, A. Shan, D. Zhang, Z. Lou, H. Yuan, X. Huang, N. Zhu, X. Hu, Dosing time of ferric chloride to disinhibit the excessive volatile fatty acids in sludge thermophilic anaerobic digestion system, Bioresource Technology 189 (2015) 154–161.
25. J.L. Chen, R. Ortiz, T.W.J. Steele, D.C. Stuckey, Toxicants inhibiting anaerobic digestion: A review, Biotechnology Advances 32 (2014) 1523–1534.
26. I. Syaichurrozi, S. Sarto, W.B. Sediawan, M. Hidayat, N. Darsono, D.S. Khaerudini, Enhancement of biogas production from sugarcane molasses-based distillery wastewater with electrocoagulation pretreatment using iron electrodes, Bioresource Technology Reports 24 (2023) 101614.
27. Z. Yu, X. Leng, S. Zhao, J. Ji, T. Zhou, A. Khan, A. Kakde, P. Liu, X. Li, A review on the applications of microbial electrolysis cells in anaerobic digestion, Bioresource Technology 255 (2018) 340–348.
28. A. Hassanein, F. Witarsa, S. Lansing, L. Qiu, Y. Liang, Bio-electrochemical enhancement of hydrogen and methane production in a combined anaerobic digester (AD) and microbial electrolysis cell (MEC) from dairy manure, Sustainability (Switzerland) 12 (2020) 8491.
29. I. Syaichurrozi, S. Sarto, W.B. Sediawan, M. Hidayat, Effect of Fe addition on anaerobic digestion process in treating vinasse: Experimental and kinetic studies, Periodica Polytechnica Chemical Engineering 67 (2023) 127–140.
30. R.E. Speece, Anaerobic biotechnology for industrial wastewater treatment, Environmental Science & Technology 17 (1983) 416A-427A.
31. X.J. Xu, W.Q. Wang, C. Chen, P. Xie, W.Z. Liu, X. Zhou, X.T. Wang, Y. Yuan, A.J. Wang, D.J. Lee, Y.X. Yuan, N.Q. Ren, The effect of PBS on methane production in combined MEC-AD system fed with alkaline pretreated sewage sludge, Renewable Energy 152 (2020) 229–236.
32. J.L. Linville, Y. Shen, R.P. Schoene, M. Nguyen, M. Urgun-Demirtas, S.W. Snyder, Impact of trace element additives on anaerobic digestion of sewage sludge with in-situ carbon dioxide sequestration, Process Biochemistry 51 (2016) 1283–1289.
33. T. Schmidt, M. Nelles, F. Scholwin, J. Pröter, Trace element supplementation in the biogas production from wheat stillage - Optimization of metal dosing, Bioresource Technology 168 (2014) 80–85.
34. I. Syaichurrozi, B. Budiyono, S. Sumardiono, Predicting kinetic model of biogas production and biodegradability organic materials: Biogas production from vinasse at variation of COD/N ratio, Bioresource Technology 149 (2013) 390–397.
35. I. Syaichurrozi, R. Rusdi, T. Hidayat, A. Bustomi, Kinetics studies impact of initial pH and addition of yeast *Saccharomyces cerevisiae* on biogas production from tofu wastewater in Indonesia, International Journal of Engineering, Transactions B: Applications 29 (2016) 1037–1046.
36. D. Wang, Z. Hao, S. Tao, Z. Shi, Z. Liu, E. Liu, S. Long, Enhanced methane production from waste activated sludge by microbial electrolysis cell assisted anaerobic digestion: Fate and effect of humic substances, Bioresource Technology 403 (2024) 130872.